



HAL
open science

Wet creep of hardened hydraulic cements - Example of gypsum plaster and implication for hydrated Portland cement

Edgar Alejandro Pachon-Rodriguez, E. Guillon, G. Houvenaghel, Jean Colombani

► To cite this version:

Edgar Alejandro Pachon-Rodriguez, E. Guillon, G. Houvenaghel, Jean Colombani. Wet creep of hardened hydraulic cements - Example of gypsum plaster and implication for hydrated Portland cement. *Cement and Concrete Research*, 2014, 63, pp.67-74. 10.1016/j.cemconres.2014.05.004. hal-02309855

HAL Id: hal-02309855

<https://univ-lyon1.hal.science/hal-02309855v1>

Submitted on 17 May 2022

HAL is a multi-disciplinary open access archive for the deposit and dissemination of scientific research documents, whether they are published or not. The documents may come from teaching and research institutions in France or abroad, or from public or private research centers.

L'archive ouverte pluridisciplinaire **HAL**, est destinée au dépôt et à la diffusion de documents scientifiques de niveau recherche, publiés ou non, émanant des établissements d'enseignement et de recherche français ou étrangers, des laboratoires publics ou privés.

Wet creep of hardened hydraulic cements - example of gypsum plaster and implication for hydrated Portland cement

Edgar Alejandro Pachon-Rodriguez^a, Emmanuel Guillon^b, Geert Houvenaghel^b, Jean Colombani^{a,*}

^a*Institut Lumière Matière; Université de Lyon; Université Claude Bernard Lyon 1; CNRS, UMR 5306; Domaine scientifique de la Doua, F-69622 Villeurbanne cedex, France*

^b*Lafarge Centre de Recherche; 95, rue du Montmurier, BP 15, F-38291 Saint Quentin Fallavier cedex, France*

Abstract

Gypsum plaster exhibits a dramatic creep when placed in a very humid environment. We have combined mechanical tests of wet bending creep of set plaster and holographic interferometry measurements of dissolution rate and diffusion coefficient to look for the origin of this wet creep. Both these experiments have been performed in absence and presence of various known anti-creep admixtures. It appears that the creep rate and dissolution rate are strongly correlated. This correlation has allowed to propose surface-driven pressure solution creep as mechanism of wet creep of gypsum plaster, i.e., the sequence dissolution in the grain boundary water/diffusion/precipitation at the grain surface. An order of magnitude analysis shows that this dissolution-diffusion-recrystallization series can also contribute to the creep of hydrated Portland cement.

*Corresponding author, jean.colombani@univ-lyon1.fr

Keywords: A: Humidity, B: microstructure, C: creep, D: admixture, dissolution

1. Introduction

Hydraulic cements are mineral powders that harden under water, and subsequently remain cohesive in presence of water. They constitute the main materials of the building industry, used under the form of pastes to enable molding in the desired shape. Portland cement and gypsum plaster are the most used hydraulic binders because of their availability, low cost and easy installation. Hardened Portland cement and its derivatives (mortar, concrete) has also the virtue to be load-bearing, and hydrated plaster of Paris to be light, isolating and fire resistant. One of their limitations is their long-time plastic strain, or creep, mainly indoor for gypsum plaster and outdoor for hardened Portland cement. For gypsum, this creep is strongly enhanced by the presence of humidity.

Being chemically and structurally much simpler than hydrated cement pastes, this study is devoted to the creep of set plaster of Paris, with the aim to identify the underlying mechanisms and to estimate their applicability to the cementitious materials. Indeed the elimination, or at least limitation, of this drawback requires the understanding of its microscopic origin. Few studies have been devoted to the investigation of the link between the microstructure and the mechanical properties of set plaster. Concerning the influence of water, the few existing studies have brought some clues for the interpretation of the stiffness and resistance of set plaster in humid or wet environments. But up to now, the creep in presence of water had not re-

23 ceived any explanation. We have proposed recently that it derives from the
24 dissolution of gypsum [1]. This finding has enabled to propose pressure so-
25 lution creep as the mechanism of wet creep of set plaster. We detail here the
26 experiments (mechanical tests and interferometric measurements) leading to
27 this result and discuss its implications for hydrated Portland cement.

28 **2. Mechanical properties of gypsum plaster in presence of water**

29 Set plaster is constituted of intricate gypsum ($\text{CaSO}_4, 2\text{H}_2\text{O}$) needles,
30 roughly $20\ \mu\text{m}$ long, obtained from the hydration of plaster of Paris ($\text{CaSO}_4, \frac{1}{2}\text{H}_2\text{O}$).
31 The cohesion of the material derives from the bonds between the needles and
32 from the tenon and mortise joints between them [2]. It has been postulated
33 about ten years ago that the bond between the needles is of the same nature
34 as the bond between flocculated colloids [3]. Therefore the gypsum micro-
35 crystallites should be linked via a nanometric water film. The attraction
36 between them should stem from van der Waals interactions between the fac-
37 ing charged faces and ionic correlations between the Debye layers developing
38 in the water close to the surface, and the repulsion from the exclusion of
39 the Debye layers. At the ends of the water layers, capillary forces develop
40 at menisci and contribute to the cohesion between the needles. The balance
41 between these forces determines the liquid film thickness. It has been added
42 a few years later that the presence of “bridging”, i.e., solid, interfaces, be-
43 side these “non-bridging” liquid interfaces between needles, is necessary to
44 obtain a more comprehensive interpretation of the set plaster properties [4].
45 This vision of the microstructure of the material enables to interpret several
46 mechanical properties of wet or humid set plaster:

- 47 • it has been observed that Young's modulus of set plaster decreases
48 when the relative humidity increases [5, 6]. This can be interpreted by
49 the fact that the equilibrium thickness of the water inter-needle layers
50 increases with the relative humidity enhancement, from ~ 1 nm in dry
51 conditions to ~ 10 nm in humid ones [3]. And a thicker layer induces
52 a weaker bond between needles. The assumption has been made that
53 this weakened connection can result in a reversible slip between some
54 microcrystallites, increasing the elastic strain, thus decreasing Young's
55 modulus. The bridging bonds deform only by elastic bending and guar-
56 antee that no irreversible strain occurs.
- 57 • The flexural strength, i.e., the bending failure stress of this brittle ma-
58 terial, has also been seen as decreasing when the material is soaked in
59 water [7] or when it adsorbs water [8]. This feature can also be ascribed
60 to the thickening of the water layers in a humid environment. Indeed
61 the resulting slip between microcrystallites implies a lower contribution
62 of the non-bridging bonds to the strength, so a lowered failure stress.
- 63 • It has also been observed that, if the hardness of a set plaster sample
64 decreases after being plunged in water, the hardness recovers its initial
65 value once the sample is dried [7]. The reversibility of the influence
66 of water can again be interpreted by the fact that the mechanical
67 resistance of the material reflects the values of the inter-needle water
68 slab thickness, in equilibrium with the quantity of water available. If
69 more water is available, the layer thickens and the cohesion diminishes,
70 and vice-versa.

71 **3. Wet creep of gypsum plaster**

72 Beside these successes of the theory, one should mention that unfortu-
73 nately it does not provide any mean to understand the increase of creep in
74 a humid environment [9, 10]. Indeed creep is a slow process occurring over
75 periods of days or months, whereas the equilibration of the intercrystalline
76 water layers is a quasi-instantaneous mechanism. Thereby the progressive
77 plastic strain occurring during creep cannot be explained by a progressive
78 increase of the slab dimension leading to a loss of cohesion.

79 We show here that the wet creep of set plaster is a consequence of a
80 phenomenon called pressure solution creep (figure 1). When an external
81 stress, or simply its own weight, is applied to a gypsum board, the gypsum
82 needles are subject to local stresses. These stresses induce an increase of the
83 chemical potential of the gypsum. So when water is present, in particular in
84 the intercrystalline contacts, to recover chemical equilibrium, the chemical
85 potential of the liquid increases also to equalize with the one of the solid. This
86 leads to the enhancement of the solubility of gypsum, thereby to a dissolution
87 of the solid in the liquid. Therefore concentration gradients appear along the
88 water layers, which induce Fick diffusion of dissolved gypsum. When the
89 sulfate and calcium ions reach areas without stress, their solubility recovers
90 its initial value and they precipitate on the solid at rest. This dissolution-
91 diffusion-precipitation series continues as long as the local stress exists, and
92 induces a transfer of matter from high stress to low stress regions. By this
93 way a plastic strain occurs, which accommodates the applied stress, and the
94 material creeps.

95 This phenomenon is well known in geology. It has been ascribed several

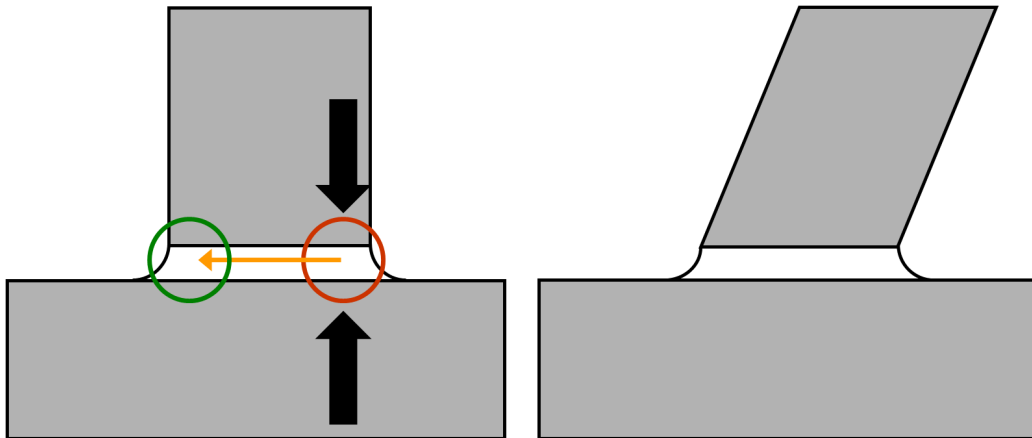


Figure 1: Sketch of the consecutive steps of pressure solution creep in gypsum plaster: an external load creates a local compression stress between two gypsum needles, which induces dissolution, diffusion of the dissolved species, and recrystallisation in a non-stressed area. This sequence induces a local transfer of matter, so a macroscopic plastic strain.

96 contributions to the upper crust evolution, for instance during non-seismic
 97 strain of active faults, or for the transformation of loose sediments into co-
 98 hesive sedimentary rocks [11]. Pressure solution creep has in particular be
 99 evidenced in wet gypsum particulates under uniaxial and hydrostatic load
 100 [12, 13].

101 Numerous experiments of pressure solution creep in water have been per-
 102 formed in laboratory, with the final aim of understanding geological situa-
 103 tions. Many of these studies use model systems or model configurations from
 104 which we can learn on the basic mechanisms and characteristic kinetics of
 105 pressure solution [11]. But their specific features, generally devoted to geol-
 106 ogy, make their application to industrial materials difficult. For instance, the
 107 available works on pressure solution in gypsum study low porosity assemblies

108 of non-cohesive quasi-spherical gypsum crystallites,. All of these character-
109 istics differ from industrial gypsum, thereby making the application of these
110 studies difficult to building materials. We have not found such a study in the
111 materials science field. Therefore a protocol enabling to validate the existence
112 of pressure solution in the creep of humid gypsum plaster is necessary.

113 Before going on, we would like to recall that it was formerly thought that
114 the decrease of the mechanical strength of set plaster with moisture could
115 be due to the dissolution of small gypsum crystals, precipitated at the end
116 of the plaster setting and bridging the gypsum needles [14, 15]. This phe-
117 nomenon was sometimes misleadingly called "dissolution-recrystallization".
118 Pressure solution creep mentioned here also involves dissolution and recryst-
119 tallization but in a totally different way: dissolution occurs at high stress
120 regions of inter-needle contacts and recrystallization at low stress regions or
121 at the needles surface. No microcrystal appears or disappears. This hypoth-
122 esis of dissolving-recrystallizing microcrystals was unambiguously discarded
123 by hardness and bending tests in various conditions of plaster setting and
124 relative humidity [7].

125 To establish a protocol of validation of the presence of pressure solution
126 creep, we benefit from the methodology of the works performed on the ge-
127 ological side. In these studies, the presence of pressure solution creep, and
128 its exact nature, is usually determined by measuring the creep kinetics. The
129 slowest step in the reaction-transport-recrystallization sequence limits the
130 matter transfer rate, so drives the whole kinetics and determines the evolu-
131 tion laws.

132 The theoretical determination of the exact expression of $\varepsilon(t)$, the strain

133 evolution with time, requires to define precisely many parameters: order of
134 the chemical reaction, reactive surface area, thickness of the liquid slab, locus
135 of the precipitation sites, porosity, size distribution of the mineral grains,
136 width of the solid contacts, ... The final $\varepsilon(t)$ curves have been found to be
137 highly dependent on the above characteristics of the system and on their
138 interplay. A particularly complete modelization of pressure solution creep in
139 sandstone for instance can be found in Ref. [16].

140 As no complete pressure solution modelization of a highly porous medium
141 like set plaster exists, we have to make with first-order models, bringing at
142 least trends of the strain evolution with time. We have chosen the acclaimed
143 model of Raj [17]. His modelization considers the creep of a unique stressed
144 cubic mineral sample in a solvent present in channels at its surface. It states
145 that :

- 146 • if the kinetics is driven by the mass transport (due in general to a low
147 flow rate of diffusion in tiny channels), the strain rate writes:

$$d\varepsilon/dt \sim \sigma D s/d^3 \quad (1)$$

- 148 • if the kinetics is driven by the surface reaction (due to its slowness),
149 the strain rate writes:

$$d\varepsilon/dt \sim \sigma k s/d \quad (2)$$

150 In these expressions, σ is the applied stress, D the diffusion coefficient of the
151 dissolved species, k the **reaction** rate constant of the mineral, s its solubility
152 and d the characteristic size of the constrained interface.

153 In geological laboratory experiments, the limiting step is estimated in
154 varying the grain size d and determining if the strain rate scales as d^{-1}

155 or d^{-3} . In our case, varying the gypsum crystallites size in set plaster is
156 difficult. To identify the limiting stage, we have benefited from the existence
157 of admixtures added to the plaster industrially to limit the humid creep.
158 These additives are efficient in slowing down the creep strain rate, but again,
159 their mechanism of action is not understood yet. So the idea of our work is to
160 find which factor of the above expressions, if any, these admixtures modify,
161 to lower the strain rate, thus indicating the working mechanism of creep.

162 4. Experiments

163 In equations 1 and 2, the parameters the knowledge of which is needed
164 are d , s , k , D and $d\varepsilon/dt$.

165 4.1. Admixtures

166 The investigated anti-creep admixtures are a tartaric acid ($C_4H_6O_6$) / boric
167 acid (H_3BO_3) mixture, Trilon P, i.e., a commercial version of a sodium salt of
168 a polyamino carboxylic acid ($C_{10}H_{16}N_2O_8$, CAS no. 454473-50-8), Sequion
169 50K33 and Dequest 2054, i.e., two commercial versions of the hexamethylene-
170 diamine tetra(methylene phosphonic acid) hexapotassium salt ($C_{10}H_{22}K_6N_2O_{12}P_4$,
171 CAS no. 38820-59-6), and STMP, i.e., sodium trimetaphosphate ($Na_3P_3O_9$).
172 The acid mixture is made of 1/6 of tartaric acid and 5/6 of boric acid in
173 weight.

174 4.2. Bend creep tests

175 For the bend tests, gypsum (from Mazan quarry, France) is ground and
176 dehydrated to make plaster ($CaSO_4, \frac{1}{2}H_2O$). The resultant powder is mixed
177 with water to make a paste with a water/plaster weight ratio of 0.8, bringing

178 a convenient compromise between the fluidity of the paste and the porosity
179 of the final product (57%). The mixture is cast in a parallelepipedic mold,
180 placed in a closed vessel during 24 h to achieve complete hydration, dried, and
181 stored in calcium sulfate saturated water until the test, to avoid dehydration
182 [15]. The same protocol was also followed with water containing the various
183 admixtures.

184 Standard bend tests have been performed to measure the creep strain rate
185 of set plaster. The above-described samples were loaded in the middle on
186 the top face and supported at their ends. The deflection was recorded with a
187 Linear Variable Differential Transformer displacement sensor every 2 h during
188 15 days. During the tests, the beams were immersed in water —to study
189 wet behavior— saturated with calcium sulfate —to avoid normal dissolution
190 and be sure to observe, if any, pressure dissolution. The maximum load
191 was chosen as 20% of the tensile strength, measured for each batch on one
192 sample before the test, to remain outside the stress range where subcritical
193 crack growth inside the samples is expected, risking to blur the results [9, 18].

194 The force and displacement are converted in the stress σ and strain ε at
195 the top face in the middle of the beam with the elastic approximation:

$$\sigma = \frac{3PL}{2wh^2} \quad \text{and} \quad \varepsilon = \frac{6h\delta}{L^2} \quad (3)$$

196 In these expressions, P is the load, L the support span, $w = 20$ mm the
197 width of the beam and $h = 20$ mm its height.

198 The zero-stress curve inside the beam may depart from the center of the
199 beam, due to non-symmetry of the compressive and tensile strain mechanism,
200 which may make these formulas non valid. But the determination of the exact
201 stress field is not possible and would deserve a study for itself.

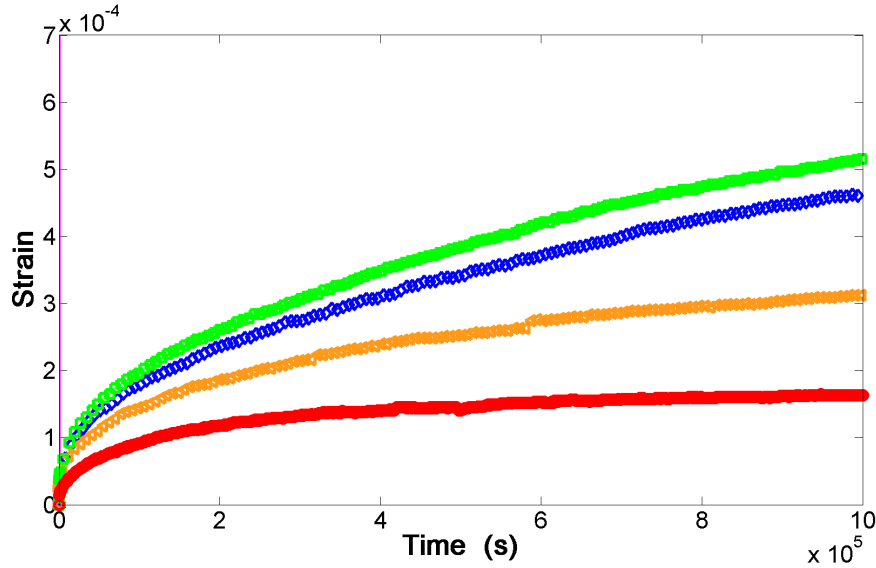


Figure 2: Evolution with time of the bending strain for the gypsum plaster samples manufactured with 0.15% Sequion **in the preparation water**. The applied stress, from the bottom to the top curve is 0.244 (red), 0.332 (orange), 0.356 (blue) and 0.386 (green) MPa.

202 An example of $\varepsilon(t)$ curves at various stresses for one admixture is shown in
 203 figure 2. The strain rate $d\varepsilon(t)/dt$, needed for the test of the above-mentioned
 204 equations is obtained in derivating the experimental $\varepsilon(t)$ curves numerically.
 205 From it, the creep compliance rate $(d\varepsilon(t)/dt)/\sigma$ is computed. **All strain-time**
 206 **data and curves for all admixtures and stresses can be found as Supplemen-**
 207 **tary Material.**

208 A parameter that may play a role in the elaboration of the samples is
 209 the concentration of admixture in the water used to manufacture the gyp-
 210 sum from the plaster powder. Several concentrations between 0.05% and
 211 0.5% in weight have been tested for each additive. The creep results have
 212 been found to be independent on the concentration, except for the smallest

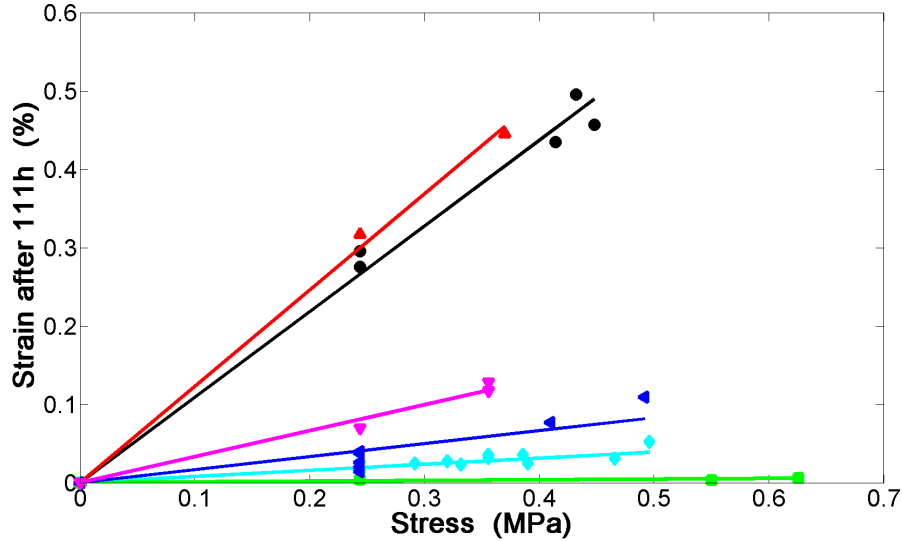


Figure 3: Bend strain ε after 111 h versus applied stress σ for the various admixtures: pure water (black circles), boric/tartaric acid (red upward triangles), Trilon (pink downward triangles), Dequest (blue leftward triangles), Sequion (light blue diamonds), STMP (green squares).

213 concentrations ($\lesssim 0.1\%$) where the anti-creep action is less efficient.

214 The strain obviously depends on the bending stress. To get an estimate
 215 of the evolution of the creep intensity with the applied stress, the value of the
 216 bend strain at one given time (namely 111h) has been drawn versus the bend
 217 stress in figure 3. It can be stated that the creep is roughly proportional to
 218 the applied stress in the range investigated in this study.

219 4.3. Contact size

220 The determination of the inter-needle contact size d is not a trivial task
 221 and for this we have performed scanning electron microscopy observations of
 222 the microstructure of the set plaster samples (figure 4). For all the admix-

223 tures used, the microstructure remains of the acicular type. None of them
224 reveal lenticular or columnar habit, sometimes encountered in natural gyp-
225 sum, depending on the impurities adsorbing on specific crystalline planes.
226 The characteristic size of the microcrystals is similar at first order in all pic-
227 tures and we have considered that the contact size d should also be similar
228 among all samples. For the computations in next section, the average value
229 of $d = 1 \mu\text{m}$ has been chosen.

230 Nevertheless we can mention that gypsum plaster elaborated with Se-
231 quion reveals unexplained micrometer-size etch pits at the needles surface.
232 Whereas we have seen that, according to the SEM pictures, the influence
233 of the additives on the set plaster microstructure is not significant, we have
234 attempted to get a further evidence of this lack of influence in testing another
235 protocol of elaboration of the samples. In this process, all solid samples are
236 first elaborated from plaster and pure water, in the absence of any admix-
237 ture. Subsequently, each sample is soaked during 12h in water containing
238 a given concentration of additive, to make the molecules impregnate the
239 gypsum crystallites network of the material. The creep bend tests are then
240 performed as detailed in section 4.2. The interest of this procedure is to
241 guarantee that all samples have strictly the same microstructure, having all
242 been elaborated in pure water.

243 Figure 5 shows the creep curves for one admixture present in the impreg-
244 nation water at various concentrations. As the applied stresses are almost
245 similar, the difference between the various curves can be ascribed to the con-
246 centration of additive in the soaking water. The more concentrated in addi-
247 tive the impregnation solution, the more efficient the anti-creep effect. The

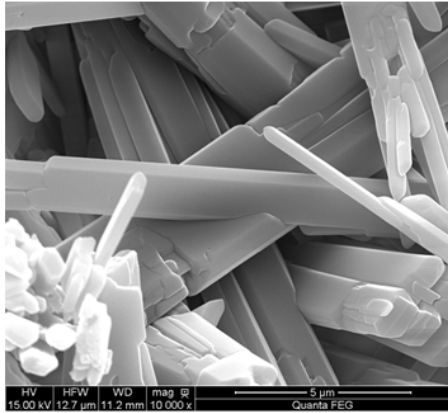
248 origin of this evolution is to be searched in the variation of the dynamics of
249 adsorption and diffusion in a porous medium of the admixture for the various
250 concentrations. This result seems to indicate that the quantity of molecules
251 inside the sample is not the same for the various concentrations, even with
252 the long impregnation time we have chosen. The adsorption and diffusion
253 dynamics may be different from one admixture to another, which makes the
254 comparison between the results obtained with the various additives quite del-
255 icate. Therefore, we have abandoned this process and exclusively used the
256 protocol presented in the previous section, where we have the certainty that
257 the molecules are embedded in the samples.

258 *4.4. Solubility*

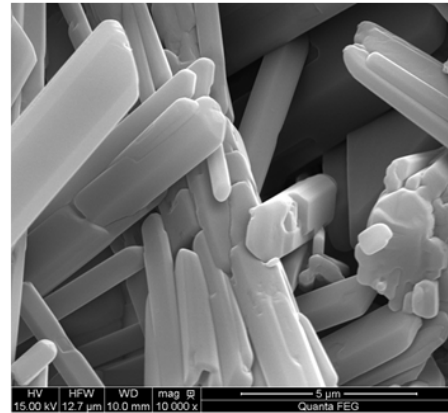
259 The solubility of gypsum in aqueous solutions of the various admix-
260 tures has been determined by induced coupled plasma atomic emission spec-
261 troscopy. Certainly due to the low concentration of additive here, no depar-
262 ture from the solubility of gypsum in pure water (2 g/L, 15 mmol/L) has
263 been found, whatever the added product.

264 *4.5. Dissolution rate constant*

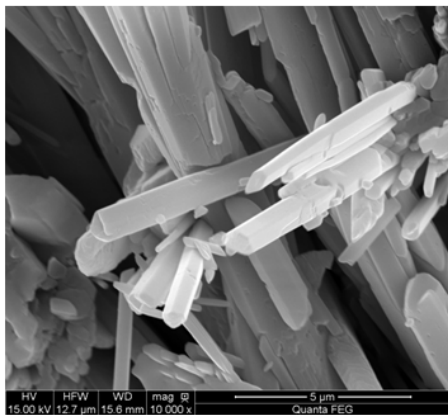
265 The gypsum-water interfacial reaction rate constant is also needed, being
266 either the dissolution or precipitation rate constant in Raj's equation. De
267 Meer and Spiers identified precipitation as the driving mechanism, which
268 can be expected in their low porosity system, where unstressed precipitation
269 sites are rare [13]. But the dissolution and precipitation rate constants should
270 be close. Indeed the rate of attachment and detachment of ions at a solid
271 surface are strongly linked, and a change of the surface reactivity influence



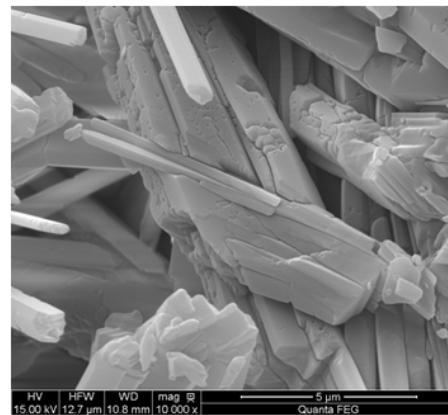
water



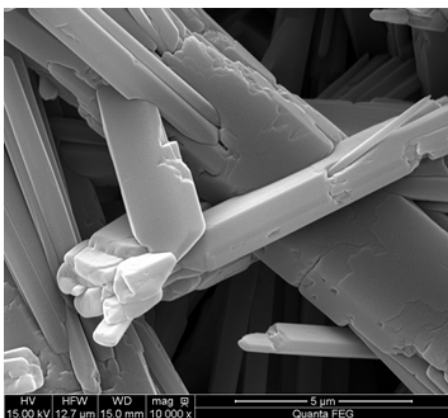
tartaric/boric acid



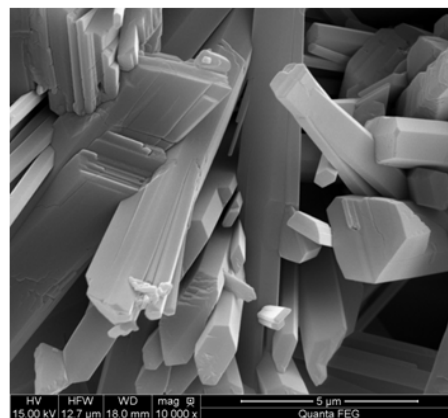
Trilon



Sequion



Dequest



STMP

Figure 4: Scanning electron microscope pictures of set plaster samples, pure and elaborated with the various admixtures. The dimension of the images is $12.7 \times 11.0 \mu\text{m}^2$.

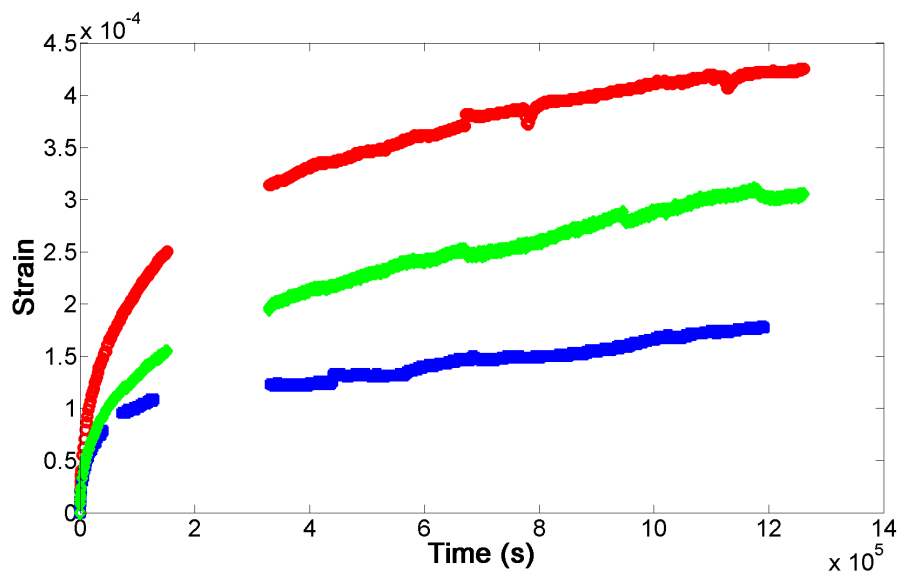


Figure 5: Evolution with time of the bending strain for the pure gypsum plaster samples impregnated by Sequion. From the top to the bottom curve, the concentration of Sequion in the impregnation water is 0.50 g/L for a 0.406 MPa stress (red), 4.97 g/L for a 0.524 MPa stress (green) and 9.94 g/L for a 0.496 MPa (blue).

272 both [19]. We have chosen to study the dissolution rate constant. But if
273 a correlation between creep and dissolution is found and shows that the
274 phenomenon is interface-driven, it is very likely that a correlation between
275 creep and precipitation also exists.

276 The measurement of the dissolution rate constant is a delicate task. As
277 we have shown in preceding studies, the usual solution chemistry methods
278 provide dissolution rates blurred by mass transport phenomena (diffusion,
279 convection) [20, 21]. As the possible effect of admixture on the dissolution
280 rate constant may be tiny, the standard dissolution measurement techniques
281 were not appropriate and we have used an alternative methodology, holo-
282 graphic interferometry. This technique has been described in detail in Ref.
283 [22]. It presents two major advantages. First the experiment is performed in
284 quiescent water, thereby avoiding any convective disturbance. Secondly the
285 concentration is directly measured at the solid-liquid interface, whereas in
286 standard methods it is measured in the flowing liquid far from the surface.

287 The dissolution rate constant k of gypsum of the same origin as in the
288 bend tests —to allow comparison— in water containing the various admix-
289 tures has been measured by holographic interferometry and for all of them,
290 k has been found to be modified by the admixture [23]. The results are
291 summarized in table 1.

292 *4.6. Diffusion coefficient*

293 The holographic interferometry experiments have also the advantage to
294 give access to the diffusion coefficient D of dissolved gypsum in water. There-
295 fore D has been measured for gypsum in water containing the various ad-
296 mixtures and it has been seen that this coefficient is almost constant for all

Admixture	k (10^{-6} mol m $^{-2}$ s $^{-1}$)	D (10^{-10} m 2 s $^{-1}$)
Without	46	7.1
Tartaric-boric acid	74	5.9
Trilon	21	4.3
Sequion	11	6.1
Dequest	8.0	4.9
STMP	3.3	6.5

Table 1: Dissolution rate constant k and diffusion coefficient D of gypsum in water containing various admixtures, measured by holographic interferometry.

297 admixtures, probably due to the low concentration of the products, as shown
298 in table 1.

299 5. Results and discussion

300 Before testing our assumption of pressure solution creep using all the
301 experiments described in the preceding section, we would like to focus first
302 on the $\varepsilon(t)$ curves. They constitute the first systematic study of the wet
303 creep of gypsum plaster. By fitting the curves, we have noticed that all of
304 them obey to a power law: $\varepsilon(t) = At^n$, with $n < 1$. Thereby, we see that
305 a consolidating mechanism is active during the wet creep, which slows down
306 progressively the strain. The creep exponent n depends on the admixture
307 with which the set plaster sample has been manufactured: 0.69 for pure
308 water, 0.71 for boric/tartaric acid, 0.52 for Trilon, 0.34 for Sequion, 0.39 for
309 Dequest and 0.38 for STMP. It is striking to state that it evolves from $\sim 2/3$
310 to $\sim 1/3$ from pure water to the most efficient anti-creep admixture. Figure
311 6 illustrates this evolution. We have not found yet the origin of this ability

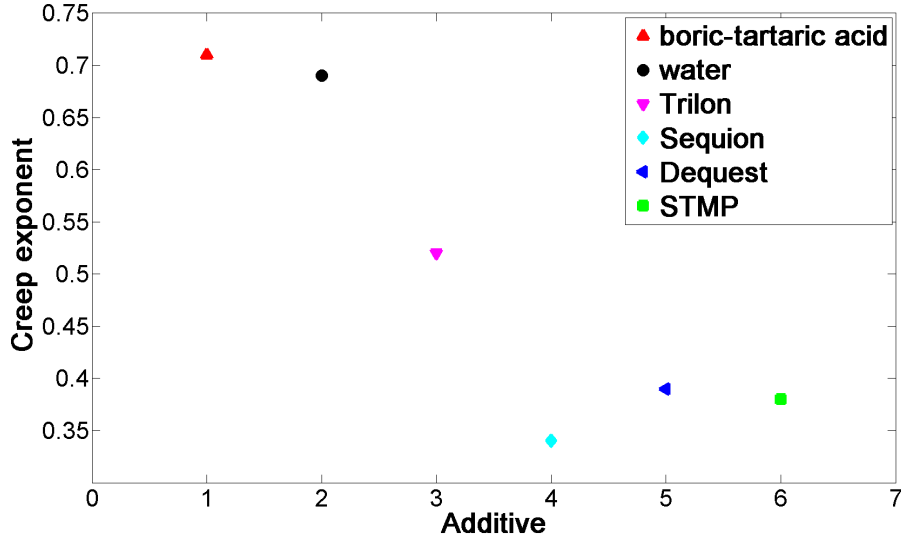


Figure 6: Bend creep exponent of wet gypsum plaster manufactured with the various admixtures.

312 of admixtures to lower the creep exponent. We can just mention that the
 313 $1/3$ exponent in presence of anti-creep products recalls both i) the exponent
 314 of Andrade creep, i.e., diffusive creep in non-porous materials, and ii) the
 315 pressure solution creep exponent observed in NaCl single crystals by Dysthe
 316 et al. [24].

317 We are now able to test the agreement between our experiments and
 318 equations 1 and 2. For the first one, we have plotted in figure 7 the creep
 319 compliance rate $\dot{\varepsilon}(t_0)/\sigma$ as a function of $D s/d^3$. **To gain statistical accuracy,**
 320 **each dot in this figure represents an average of the results of a few experiments**
 321 **performed at quasi-equal stresses.** The question of the choice of t_0 arises.
 322 Indeed the $\varepsilon(t)$ curves are non linear. We have chosen $t_0 = 1 \times 10^5$ s, in
 323 the middle of the investigated time, but we have checked otherwise that the

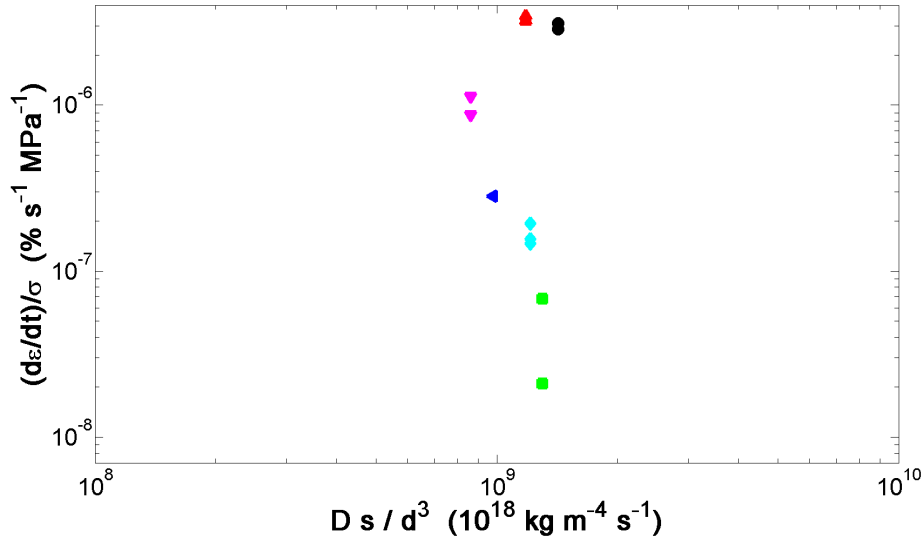


Figure 7: Compliance rate for wet bending creep of gypsum plaster elaborated with a given additive at $t_0 = 1 \times 10^5$ s, as a function of a coefficient proportional to the diffusion coefficient of dissolved gypsum in a solution of the same additive. Red upward-pointing triangles: tartaric/boric acid; black circles: pure water; pink downward-pointing triangles: Trilon; blue left-pointing triangles: Sequoin; light blue diamonds: Dequest; green squares: STMP.

324 obtained correlation is valid all along the experiments. As can be seen in
 325 figure 7, no correlation is observable between the 2 factors. The compliance
 326 rate varies of 2 orders of magnitude among the admixtures, whereas the
 327 diffusion coefficient remains almost constant (s and d keeping always the
 328 same value). Therefore the diffusion velocity of the gypsum dissolved species
 329 has no influence on the creep kinetics, which discards the diffusion-driven
 330 pressure solution creep as creep mechanism.

331 Now, to test equation 2, we have drawn in figure 8 the creep compliance
 332 rate $\dot{\epsilon}(t_0)/\sigma$ as a function of $k s/d$. Again, each dot in the figure stands for an

333 average of the results of a few experiments performed at close stresses. Here
334 we see a very strong correlation between the two quantities. Indeed $\dot{\epsilon}(t_0)$
335 and k evolve of almost 2 orders of magnitude from pure water to the most
336 efficient anti-creep coefficient, giving rise to the observed coupling between
337 the two parameters in figure 8. This correlation is a strong support to the fact
338 that the wet creep of gypsum plaster is a reaction-driven pressure solution
339 creep. Again the correlation is shown at $t_0 = 1 \times 10^5$ s in figure 8 but we
340 have checked that the correlation exists all along the experiments. If the
341 link between dissolution velocity and creep velocity is established, we have
342 to mention that the first order model of the phenomenon we have used (in
343 absence of a more complete model) does not catch the exact correlation. The
344 model predicts $\dot{\epsilon} \sim (\sigma ks/d)^m$ with $m = 1$ and we find $m = 1.3$ to 1.7 , slightly
345 evolving between the beginning and the end of the experiment.

346 We would like to mention here the compressive creep tests performed by
347 Hoxha et al. with natural gypsum rocks [25]. They mention that the duration
348 of their experiments is too short (~ 15 days) to evidence pressure solution.
349 Therefore they explain the expansion of their samples by a mechanism of
350 reversible migration of water molecules, from the solid to the pore space. As
351 shown here, the consequence of pressure solution creep may be observable
352 even for such short period of time. **With the material at hand, we are not able
353 to explain why they do not observe precipitation-limited pressure solution
354 creep like de Meer & Spiers with a system of similar porosity [13].**

355 Now that the basic mechanism of the wet creep of gypsum plaster is
356 elucidated, a detailed theoretical analysis of pressure solution in an as porous
357 material as gypsum plaster would enable to make quantitative predictions

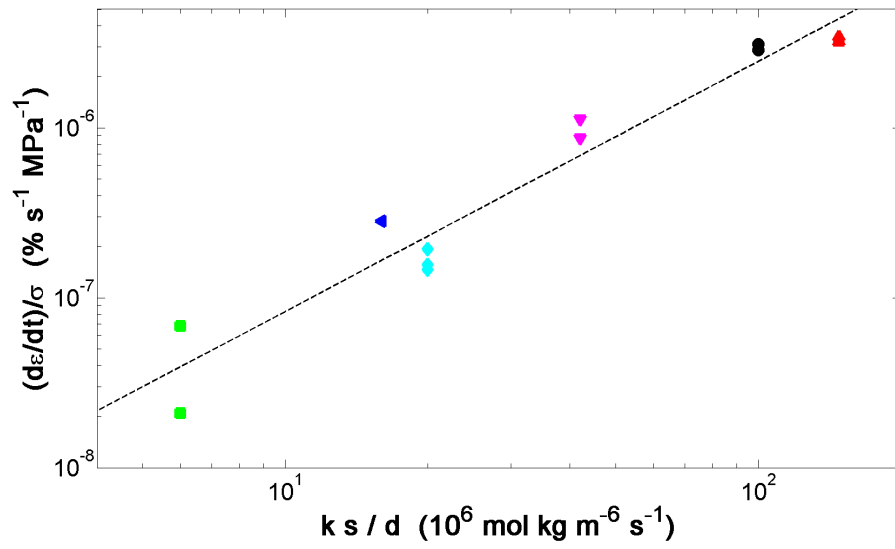


Figure 8: Compliance rate for wet bending creep of gypsum plaster elaborated with a given additive at $t_0 = 1 \times 10^5$ s, as a function of a coefficient proportional to the dissolution rate constant of gypsum in a solution of the same additive. The color code is the same as in figure 7. The black dashed line is a linear fit of the data.

358 about its kinetics. But knowing that the dissolution kinetics is at the basis
359 of wet creep enables to try to find tools against this drawback of the material.

360 **6. Implications for hydrated Portland cement**

361 Despite being the manufactured material most used on earth, the struc-
362 ture and cohesion of hydrated Portland cement is not perfectly understood
363 yet. Along a schematic view, a hydrated Portland cement paste can be con-
364 sidered as a flocculated colloidal suspension of calcium-silicate-hydrate (C-S-
365 H), i.e., $(\text{CaO})_{1.7}(\text{SiO}_2)(\text{H}_2\text{O})_{1.8}$ [26], nanometric particles, called gel, with
366 partial crystallinity [27]. $\text{Ca}(\text{OH})_2$ nanocrystallites, and other minor hydra-
367 tion products, are also present in the gel. Like in standard colloidal gels, the
368 remarkable strength of this hydraulic cement stems from electrostatic and
369 ionic correlation forces between the particles via the water layers between
370 them [28]. Capillary forces contribute also in unsaturated materials, where
371 water-air menisci are present.

372 It is generally admitted that C-S-H is found in hydrated pastes in 2 or
373 3 forms, of identical chemical composition, but clearly distinct organizations
374 and densities [3, 29, 30]. The proportion of these phases varies with the
375 water/cement ratio used to manufacture the cement paste, the drying, and
376 the aging of the material. This structural heterogeneity induces a multi-scale
377 porosity, also evolving with the just-mentioned parameters.

378 One major concern about cementitious materials is their aging, in the
379 form of shrinkage, creep, fractures, ... partly due to the slow drying of the
380 products of cement hydration [31]. It has been shown that the concrete creep
381 strain results exclusively from the irreversible strain of the cement hydration

382 products [32] and the creep of hardened cement is still an active field of
383 research [30].

384 We discuss here only about wet creep, i.e., the plastic strain under small
385 load of the water saturated material. In these conditions, capillary menisci
386 inside the material are absent, which suppresses a major source of aging of
387 the material. Therefore in this case the creep cannot derive from shrinkage
388 induced by water loss, and corresponding models do not apply [31]. Recent
389 assumptions of creep origin applying in this situation are: reorganization
390 of high density phase globules, analog to dislocation migration in crystals
391 [29], reorganization of C-S-H particles, leading to an increase of the packing
392 factor of the 3 phases, analog to granular matter flow [30], better alignment
393 of C-S-H sheets, analog to house-of-card collapse [32], ...

394 All of these hypotheses rely on the sliding of C-S-H nanoparticles, or of
395 C-S-H sheets, enabling reorganization [33]. An alternative proposal, beside
396 sliding, has also been made to explain the relative motion of C-S-H particles.
397 The possibility of the existence of the dissolution-diffusion-recrystallisation
398 series, leading to a transfer of matter among the C-S-H particles, inducing
399 plastic strain, has also been proposed [3]. Theoretical predictions of hydrat-
400 ing concrete creep have even been proposed [34, 35]. But these analytic laws
401 are phenomenological and postulate a priori the existence of a significant in-
402 fluence of the applied stress on the dissolution of the hardened material. We
403 have shown here that this influence is significant and measurable in the case
404 of wet gypsum and want to discuss here the case of hydrated cement.

405 Hydrated cement pastes share common characteristics with gypsum plas-
406 ter: They both simultaneously shrink and harden during drying, they swell

407 when immersed in water after setting, and they experience humid creep. The
 408 question of the existence of pressure solution in saturated hardened cement
 409 arises. As for gypsum, a direct observation is not possible for the moment
 410 and correlations have to be sought. Recent C-S-H nanoindentation measure-
 411 ments have shown a logarithmic creep [30]. As no comprehensive model of
 412 pressure solution creep exists, it is unfortunately not possible to draw any
 413 conclusion about pressure solution from this logarithmic evolution of the
 414 strain [11]. The order of magnitude of the creep compliance rate in these ex-
 415 periments evolves from 10^{-9} to 10^{-10} % s⁻¹ MPa⁻¹, for **samples ages similar**
 416 **to ours (~ 10 days)**. In our experiments with gypsum plaster, its values is
 417 about 10^{-6} % s⁻¹ MPa⁻¹ (figure 8).

418 The crystallites in C-S-H are nanometric. The inter-particle contact
 419 length is therefore of the same order of magnitude or lower, so 3 orders
 420 of magnitude smaller than in set plaster, where it is micrometric (figure 4).
 421 Therefore if pressure solution plays a role, the mass transport time between
 422 particles should be negligible and the phenomenon should be reaction-driven,
 423 as in the case of gypsum, and depend on the dissolution rate constant of the
 424 material via equation 2.

425 Making the first order assumption that the correlation in gypsum plaster
 426 and hydrated cement pastes are similar, we should have $(\dot{\epsilon}/\sigma)_{\text{C-S-H}}/(\dot{\epsilon}/\sigma)_{\text{gypsum}} \sim$
 427 $(ks/d)_{\text{C-S-H}}/(ks/d)_{\text{gypsum}}$. Let us review the parameters in this equation.
 428 The solubilities of the hydrated phases of cement depend highly on the na-
 429 ture and structure of the phase and on the chemical environment. But the
 430 order of magnitude of the solubility of calcium has been measured as 10
 431 mmol/L, comparable to the 15 mmol/L solubility of calcium in the case of

432 gypsum [36]. The creep compliance rate $\dot{\epsilon}/\sigma$ of hardened cement mentioned
433 above are 3 orders of magnitude lower than the one of gypsum plaster. The
434 characteristic size d of the interface between C-S-H particles is also 3 orders
435 of magnitude lower than in gypsum plaster.

436 Therefore, a dissolution rate constant of $k_{\text{C-S-H}} \sim 10^{-6} k_{\text{gypsum}} \sim 10^{-11}$
437 $\text{mol m}^{-2} \text{s}^{-1}$ would enable to explain the change in the nanoparticle struc-
438 ture responsible for the creep observed in the experiments of Vandamme &
439 Ulm [30]. Measurements with radiotracers of the dissolution rate of C-S-H
440 suspensions in aqueous solutions have brought a value $k_{\text{C-S-H}} \sim 3 \times 10^{-12}$
441 $\text{mol m}^{-2} \text{s}^{-1}$ [37]. This value is of the same order of magnitude as the value
442 we think necessary to make pressure solution active during C-S-H creep.
443 Therefore this order of magnitude analysis brings pressure solution among
444 the possible phenomena acting in the creep of C-S-H.

445 We would like to stress on the fact that our assumption is consistent with
446 all the creep models mentioned above. The novelty does not lie in the ge-
447 ometry of the motion of the nanoparticles, but in the way of this motion,
448 dissolution-recrystallisation instead of sliding. To strengthen this hypothe-
449 sis, the measurement of the dissolution rate constant of C-S-H, and other
450 hydrated phases, in aqueous solutions representative of the liquid present
451 in the nanopores of hardened cement are highly desirable, essential to base
452 on experimental evidence the contribution of pressure solution to concrete
453 creep. Besides, if the role of dissolution is corroborated, its exact role on the
454 creep strain will have to be specified. For instance, whether the dissolution-
455 diffusion-precipitation sequence results in a creep strain accomodating the
456 stress like in gypsum plaster [3], or the dissolution induces a thinning of the

457 crystallites inducing a viscoelastic strain progressively increasing with time
458 [35], will have to be clarified.

459 **7. Conclusion**

460 We have performed wet bending creep tests to measure the strain rate of
461 set plaster manufactured with various anti-creep admixtures (boric/tartaric
462 acid, Trilon, Sequion, Dequest, STMP). Besides we have carried out holo-
463 graphic interferometry experiments to measure the dissolution rate constant
464 of gypsum in water containing these anti-creep admixtures, and the diffusion
465 coefficient of dissolved gypsum in these solutions. A strong correlation has
466 been found between the wet creep strain rate and the dissolution rate con-
467 stant of the material. This clear dissolution-creep link has enabled to propose
468 reaction-driven pressure solution creep as the underlying mechanism of the
469 wet creep of gypsum plaster. This is the first time that this phenomenon is
470 evidenced **experimentally in an industrial material**.

471 Following the study of gypsum plaster, an order of magnitude analysis
472 has shown that pressure solution may also contribute to the creep of hydrated
473 Portland cement. Indeed, alternatively to the sliding between the hydrated
474 phase nanoparticles, the dissolution-diffusion-recrystallization sequence was
475 shown to be another mean of the reorganization of the nanoparticles during
476 creep.

477 **Acknowledgements**

478 We thank Elisabeth Charlaix, Ellis Gartner, François Renard et Dag Dys-
479 the for fruitful discussions. This work was supported by Lafarge Centre de

480 Recherche, Région Rhône-Alpes and CNES (french spatial agency).

481 **References**

- 482 [1] E. Pachon-Rodriguez, E. Guillon, G. Houvenaghel, J. Colombani, Pres-
483 sure solution as origin of the humid creep of a mineral material, *Phys.*
484 *Rev. E* 84 (2011) 066121.
- 485 [2] Z. Chen, S. Sucech, K. Faber, A hierarchical study of the mechanical
486 properties of gypsum, *J. Mater. Sci.* 45 (2010) 4444.
- 487 [3] J. Chappuis, A model for a better understanding of the cohesion of
488 hardened hydraulic materials, *Colloids Surf. A* 156 (1999) 223.
- 489 [4] E. M. Gartner, Cohesion and expansion in polycrystalline solids formed
490 by hydration reactions - the case of gypsum plasters, *Cem. Concr. Res.*
491 39 (2009) 289.
- 492 [5] M. Sâadaoui, S. Meille, P. Reynaud, G. Fantozzi, Internal friction study
493 of water effect on set plaster, *J. Eur. Ceram. Soc.* 25 (2005) 3281.
- 494 [6] E. Badens, S. Veessler, R. Boistelle, D. Chatain, Relation between
495 young's modulus of set plaster and complete wetting of grain bound-
496 aries by water, *Colloids Surf. A* 156 (1999) 373.
- 497 [7] P. Coquard, R. Boistelle, Water and solvent effects on the strength of
498 plaster, *Int. J. Rock Mech. Min. Sci. & Geomech. Abstr.* 31 (1994) 517.
- 499 [8] H. Andrews, The effect of water contents on the strength of calcium
500 sulfate plaster products, *J Soc. Chem. Ind.* 5 (1946) 125.

- 501 [9] H. Sattler, Elastic and plastic deformations of plaster units under uni-
502 axial compressive stress, *Mater. Struct.* 7 (1974) 159.
- 503 [10] W. Craker, K. Schiller, Plastic deformation of gypsum, *Nature* 193
504 (1962) 672.
- 505 [11] J. Gratier, D. Dysthe, F. Renard, The role of pressure solution creep in
506 the ductility of the earths upper crust, *Adv. Geophys.* 54 (2013) 47.
- 507 [12] S. deMeer, C. Spiers, Creep of wet gypsum aggregates under hydrostatic
508 loading conditions, *Tectonophys.* 245 (1995) 171.
- 509 [13] S. deMeer, C. Spiers, Uniaxial compaction creep of wet gypsum aggre-
510 gates, *J. Geophys. Res.* 102 (1997) 875.
- 511 [14] M. Murat, L. Pusztaszeri, M. Gremion, Corrélation texture cristalline-
512 propriétés mécaniques de plâtres durcis. étude préliminaire, *Mater.*
513 *Struct.* 8 (1974) 377.
- 514 [15] A. Lewry, J. Williamson, The setting of gypsum plaster Part II The
515 development of microstructure and strength, *J. Mater. Sci.* 29 (1994)
516 5524.
- 517 [16] F. Renard, D. Dysthe, J. Feder, K. Bjorlykke, B. Jamtveit, Enhanced
518 pressure solution creep rates induced by clay particles: Experimental
519 evidence in salt aggregates, *Geophys. Res. Lett.* 28 (2001) 1295–1298.
- 520 [17] R. Raj, Creep in polycrystalline aggregates by matter transport through
521 a liquid phase, *J. Geophys. Res.* 87 (1982) 4731.

- 522 [18] S. Meille, M. Sâadaoui, P. Reynaud, G. Fantozzi, Mechanisms of crack
523 propagation in dry plaster, *J. Eur. Ceram. Soc.* 23 (2003) 3105.
- 524 [19] A. Lasaga, A. Luttge, A model for crystal dissolution, *Eur. J. Mineral.*
525 15 (2003) 603.
- 526 [20] J. Colombani, Measurement of the pure dissolution rate constant of a
527 mineral in water, *Geochim. Cosmochim. Acta* 72 (2008) 5634.
- 528 [21] J. Colombani, Dissolution measurement free from mass transport, *Pure*
529 *Appl. Chem.* 85 (2013) 61.
- 530 [22] J. Colombani, J. Bert, Holographic interferometry study of the dissolu-
531 tion and diffusion of gypsum in water, *Geochim. Cosmochim. Acta* 71
532 (2007) 1913.
- 533 [23] E. Pachon-Rodriguez, J. Colombani, Pure dissolution kinetics of an-
534 hydrite and gypsum in inhibiting aqueous salt solutions, *AIChE J.* 59
535 (2013) 1622.
- 536 [24] D. Dysthe, Y. Podladchikov, F. Renard, J. Feder, B. Jamtveit, Universal
537 scaling in transient creep, *Phys. Rev. Lett.* 89 (2002) 246102.
- 538 [25] D. Hoxha, F. Homand, C. Auvray, Deformation of natural gypsum rock:
539 Mechanisms and questions, *Eng. Geol.* 86 (2006) 1.
- 540 [26] A. Allen, J. Thomas, H. Jennings, Composition and density of nanoscale
541 calcium-silicate-hydrate in cement, *Nature materials* 6 (2007) 311.

- 542 [27] R. J. M. Pellenq, A. Kushima, R. Shahsavari, K. J. Van Vliet, M. J.
543 Buehler, S. Yip, F.-J. Ulm, A realistic molecular model of cement hy-
544 drates, *Proc. Nat. Acad. Sci. USA* 106 (2009) 16102.
- 545 [28] A. Gmira, M. Zabat, R. Pellenq, H. V. Damme, Microscopic physical
546 basis of the poromechanical behavior of cement-based materials, *Mater.*
547 *Struct.* 37 (2004) 3.
- 548 [29] H. Jennings, Colloid model of C-S-H and implications to the problem
549 of creep and shrinkage, *Mater. Struct.* 37 (2004) 59.
- 550 [30] M. Vandamme, F. Ulm, Nanogranular origin of concrete creep, *Proc.*
551 *Nat. Acad. Sci. USA* 106 (2009) 10552.
- 552 [31] Z. Bazant, Prediction of concrete creep and shrinkage: past, present
553 and future, *Nuclear Eng. Design* 203 (2001) 27.
- 554 [32] P. Acker, Swelling, shrinkage and creep: a mechanical approach to
555 cement hydration, *Mater. Struct.* 37 (2004) 237.
- 556 [33] J. Sanahuja, L. Dormieux, Creep of a C-S-H gel: a micromechanical
557 approach, *Int. J. Multiscale Comput. Eng.* 357 (8) 2010.
- 558 [34] Z. Grasley, D. Lange, Constitutive modeling of the aging viscoelastic
559 properties of portland cement paste, *Mech. Time-Depend. Mater.* 11
560 (2007) 175.
- 561 [35] M. Suter, G. Benipal, Constitutive model for aging thermoviscoelasticity
562 of reacting concrete ii: results and discussion, *Mech. Time-Depend.*
563 *Mater.* 14 (2010) 291.

- 564 [36] J. Chen, J. Thomas, H. Taylor, H. Jennings, Solubility and structure of
565 calcium silicate hydrate, *Cem. Concr. Res.* 34 (2004) 1499.
- 566 [37] I. Baur, P. Keller, D. Mavrocordatos, B. Wehrli, C. Johnson,
567 Dissolution-precipitation behaviour of ettringite, monosulfate, and cal-
568 cium silicate hydrate, *Cem. Concr. Res.* 34 (2004) 341.